




Article

Enzymatic Redox Properties and Cytotoxicity of Irreversible Nitroaromatic Thioredoxin Reductase Inhibitors in Mammalian Cells

Aušra Nemeikaitė-Čėnienė¹, Lina Misevičienė², Audronė Marozienė², Violeta Jonušienė³ 
and Narimantas Čėnas^{2,*}

- ¹ Department of Immunology of State Research Institute Center for Innovative Medicine, Santariškių St. 5, LT-08406 Vilnius, Lithuania; ausra.ceniene@imcentras.lt
- ² Department of Xenobiotics Biochemistry, Institute of Biochemistry of Vilnius University, Sauletekio 7, LT-10257 Vilnius, Lithuania; lina.miseviciene@bchi.vu.lt (L.M.); audrone.maroziene@bchi.vu.lt (A.M.)
- ³ Department of Biochemistry and Molecular Biology, Institute of Biosciences of Vilnius University, Sauletekio 7, LT-10257 Vilnius, Lithuania; violeta.jonusiene@gf.vu.lt
- * Correspondence: narimantas.cenas@bchi.vu.lt; Tel.: +370-5-2234392

Abstract: NADPH:thioredoxin reductase (TrxR) is considered a potential target for anticancer agents. Several nitroheterocyclic sulfones, such as Stattic and Tri-1, irreversibly inhibit TrxR, which presumably accounts for their antitumor activity. However, it is necessary to distinguish the roles of enzymatic redox cycling, an inherent property of nitroaromatics (ArNO₂), and the inhibition of TrxR in their cytotoxicity. In this study, we calculated the previously unavailable values of single-electron reduction potentials of known inhibitors of TrxR (Stattic, Tri-1, and 1-chloro-2,4-dinitrobenzene (CDNB)) and inhibitors identified (nitrofurans NSC697923 and nitrobenzene BTB06584). These calculations were according to the rates of their enzymatic single-electron reduction (PMID: 34098820). This enabled us to compare their cytotoxicity with that of model redox cycling ArNO₂. In MH22a and HCT-116 cells, Tri-1, Stattic, CDNB, and NSC697023 possessed at least 10-fold greater cytotoxicity than can be expected from their redox cycling activity. This may be related to TrxR inhibition. The absence of enhanced cytotoxicity in BTB06548 may be attributed to its instability. Another known inhibitor of TrxR, tetryl, also did not possess enhanced cytotoxicity, probably because of its detoxification by DT-diaphorase (NQO1). Apart from the reactions with NQO1, the additional mechanisms influencing the cytotoxicity of the examined inhibitors of TrxR are their reactions with cytochromes P-450. Furthermore, some inhibitors, such as Stattic and NSC697923, may also inhibit glutathione reductase. We suggest that these data may be instrumental in the search for TrxR inhibitors with enhanced cytotoxic/anticancer activity.

Keywords: nitroaromatic compounds; cytotoxicity; oxidative stress; thioredoxin reductase; inhibition of



Citation: Nemeikaitė-Čėnienė, A.; Misevičienė, L.; Marozienė, A.; Jonušienė, V.; Čėnas, N. Enzymatic Redox Properties and Cytotoxicity of Irreversible Nitroaromatic Thioredoxin Reductase Inhibitors in Mammalian Cells. *Int. J. Mol. Sci.* **2023**, *24*, 12460. <https://doi.org/10.3390/ijms241512460>

Academic Editor: Valentina Gandin

Received: 28 June 2023

Revised: 20 July 2023

Accepted: 3 August 2023

Published: 5 August 2023



Copyright: © 2023 by the authors. Licensee MDPI, Basel, Switzerland. This article is an open access article distributed under the terms and conditions of the Creative Commons Attribution (CC BY) license (<https://creativecommons.org/licenses/by/4.0/>).

1. Introduction

Nitroaromatic compounds (ArNO₂) are widely used as antiparasitic, antibacterial, anti-tumor, and radiosensitizer agents ([1–5] and references therein). Frequently, these activities of ArNO₂ are exerted through their single-electron enzymatic reduction with the formation of radical anions (ArNO₂^{•−}) or through a two/four-electron reduction with the formation of hydroxylamines (ArNHOH). The former reaction, carried out by flavoenzyme electron-transferases, e.g., NADPH:cytochrome P-450 reductase (P-450R) or ferredoxin-type FeS proteins [6–8], initiates the redox cycling of ArNO₂^{•−} and causes oxidative stress-type cytotoxicity. The latter reaction, catalyzed mainly by NAD(P)H:quinone oxidoreductase (DT-diaphorase, NQO1) in mammalian cells, leads to the alkylation of DNA and other cellular nucleophiles [9,10]. Another relevant type of redox transformation of ArNO₂ is its denitration catalyzed by cytochromes P-450 with the formation of corresponding hydroxy

derivatives [11,12]. The reaction intermediates, epoxides, react with thiol groups. Other modes of cytotoxic and therapeutic action of ArNO_2 , in particular those associated with inhibiting certain enzymes, are discussed in recent reviews [5,13].

In this context, NADPH:thioredoxin reductase (TrxR) is considered a potential target for anticancer agents because it is overexpressed in numerous cancer lines [14–17]. Mammalian TrxRs have three cofactors in their active center: FAD, catalytic disulfide, and selenylsulfide. Selenylsulfide is located at the C-end of the protein. The physiological substrates of TrxRs are 10–12 kD disulfide proteins called thioredoxins (Trxs), which perform antioxidant and other numerous physiological functions [18]. During catalysis, the redox equivalents are transferred in the following sequence: $\text{NADPH} \rightarrow \text{FAD} \rightarrow \text{catalytic disulfide} \rightarrow \text{selenylsulfide}$. Subsequently, selenylsulfide reduces Trx or the artificial oxidant 5,5'-dithiobis(2-nitrobenzoic acid) (DTNB). The maximal reduction rate of selenylsulfide is close to that of Trx reduction [19].

Typically, TrxRs slowly reduce various groups of ArNO_2 in a one- or two-electron way, with FAD and/or catalytic selenylsulfide involved in the reactions [20–22]. On the other hand, several nitroheterocyclic compounds containing a sulfone group, such as Stattic and Tri-1 (Figure 1) or their derivatives, rapidly and irreversibly inhibit TrxR, which presumably accounts for their antitumor activity [22,23]. The therapeutic potential of Tri-1 and Stattic has been demonstrated in several non-tumor cell lines and human tumor xenografts in mice [23,24].

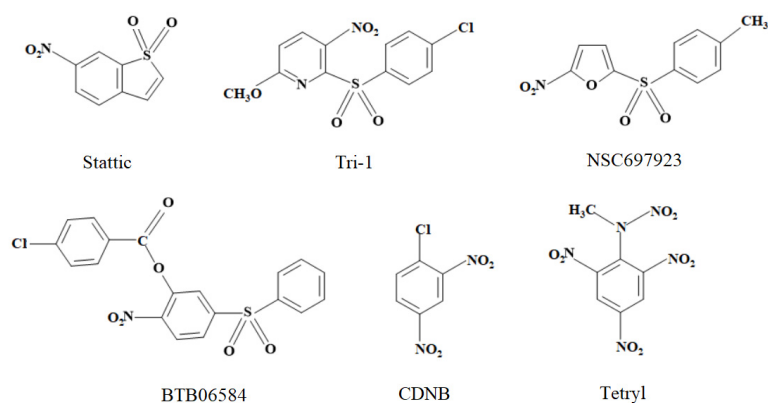


Figure 1. The structures of nitroaromatic compounds studied in this work.

However, to the best of our knowledge, redox activity and redox cycling are inherent properties of nitroaromatics, which have not been studied for the above compounds. Therefore, it is important to determine whether and to what extent TrxR inactivation increases their cytotoxicity compared to their non-specific cytotoxicity, which is mainly caused by redox cycling.

In this work, we examined the kinetics of the single-electron enzymatic reduction in Stattic and Tri-1. This allowed us to quantitatively characterize their redox cycling properties. For comparison, we studied the representatives of other groups of nitroaromatic sulfones: an inhibitor of ubiquitin-conjugating enzymes, nitrofurans NSC697923 [25,26], and an inhibitor of ATP-ase, nitrobenzene derivative BTB06584 [27]. Additionally, we investigated two well-known irreversible nitroaromatic inhibitors of TrxR, 1-chloro-2,4-dinitrobenzene (CDNB) and tetryl [20,21], which do not have a sulfonic group (Figure 1). Further enzymatic and mammalian cell cytotoxicity studies enabled us to conclude that the cytotoxicity of Stattic, Tri-1, NSC697923, and CDNB significantly exceeds the limits predicted by their redox cycling activity. This enhanced cytotoxicity may be attributed to the inhibition of TrxR. However, some additional cytotoxicity mechanisms of these compounds may also be considered.

2. Results

2.1. Enzymatic Redox Properties of Examined Nitroaromatic Compounds

It is commonly accepted that if the main cytotoxicity factor of ArNO_2 is the formation rate of $\text{ArNO}_2^- \cdot$ and their redox cycling, their cytotoxicity may be described by a general quantitative structure-activity relationship:

$$\log cL_{50} = a - b E^1_7 - c \log P (\log D), \quad (1)$$

where E^1_7 is the midpoint redox potential of the $\text{ArNO}_2/\text{ArNO}_2^- \cdot$ couple (single-electron reduction potential at pH 7.0), cL_{50} is the compound concentration causing 50% cell death or an analogous quantitative parameter, $\log P$ is the octanol/water partition coefficient, and $\log D$ is the octanol/water distribution coefficient at pH 7.0 [28–30]. These dependencies mirror the linear \log (rate constant) vs. E^1_7 relationships in a single-electron reduction of ArNO_2 by P-450R or other single-electron transferring flavoenzymes [6,30]. One may suppose that exceeding the limits predicted by the redox cycling activity may point to additional mechanisms of cytotoxicity or therapeutic action of ArNO_2 . These mechanisms might include direct or bioreductively activated alkylation, DNA intercalation, or the inhibition of particular enzymes [13].

We evaluated the unavailable E^1_7 values of tested nitroaromatics (Figure 1), as previously, by studying their single-electron reduction kinetics by P-450R and the Fe_2S_2 redox protein adrenodoxin (ADX) [31]. Flavoenzyme NADPH:adrenodoxin reductase (ADR) reduces ArNO_2 in a single-electron way, but the process is slow due to the inhibition of the reaction by excess NADPH. ADX eliminates the inhibition by NADPH and confers an additional reduction pathway via reduced ADX [32]. In both enzymatic systems, the \log of the steady-state bimolecular reduction rate constants (k_{cat}/K_m) of ArNO_2 linearly increases with E^1_7 [31]. This may be attributed to an “outer-sphere” electron transfer mechanism, where the reactivity of homologous compounds is insignificantly influenced by their structural peculiarities [33]. Thus, the unavailable E^1_7 values of ArNO_2 may be predicted from their $\log k_{\text{cat}}/K_m$, whereas their geometric average obtained in several systems ($\log k_{\text{cat}}/K_m(\text{avge})$) improves the prediction accuracy [31].

In P-450R-catalyzed reactions, the reaction rates were proportional to the concentration of NSC697923 and BTB06548 up to the limits of their solubility, 70 μM and 200 μM for other compounds. The reduction rates by ADR/ADX exhibited parabolic dependence on their concentration, giving a k_{cat} of 3.5–4.0 s^{-1} , which was close to 50% of the ADX-mediated cytochrome *c* reduction rate. The k_{cat}/K_m values of ArNO_2 reduction are given in Table 1.

Table 1. The bimolecular rate constants of reduction in nitroaromatics by NADPH:cytochrome P-450 reductase (P-450R), adrenodoxin reductase/adrenodoxin (ADR/ADX), and NAD(P)H:quinone oxidoreductase (NQO1) (0.1 M K-phosphate, pH 7.0, 25 °C), and their calculated E^1_7 values ($E^1_{7(\text{calc.})}$).

Compound	k_{cat}/K_m ($\text{M}^{-1}\text{s}^{-1}$)			$E^1_{7(\text{calc.})}$ (V)
	P-450R	ADR/ADX	NQO1	
1-Chloro-2,4-dinitrobenzene	$1.7 \pm 0.1 \times 10^5$	$3.6 \pm 0.2 \times 10^5$	$\leq 10^2$ (≤ 0.1) ^a	−0.285
NSC697923	$5.0 \pm 0.4 \times 10^4$	$1.1 \pm 0.1 \times 10^6$	$2.5 \pm 0.4 \times 10^3$ (≤ 0.25) ^a	−0.287
Stattic	$1.3 \pm 0.1 \times 10^5$	$1.6 \pm 0.1 \times 10^5$	$6.8 \pm 0.8 \times 10^2$ (0.15 ± 0.02) ^a	−0.304
BTB06584	$1.6 \pm 0.1 \times 10^4$	$3.7 \pm 0.2 \times 10^5$	(≤ 0.07) ^b	−0.326
Tri-1	$1.7 \pm 0.1 \times 10^4$	$3.7 \pm 0.2 \times 10^4$	$2.1 \pm 0.2 \times 10^3$ (0.10 ± 0.02) ^a	−0.365

^a The values of k_{cat} (s^{-1}) are given in parentheses, ^b rate at the solubility limit of BTB06548, 70 μM .

The previously determined $\log k_{\text{cat}}/K_m(\text{avge})$ of model ArNO_2 in P-450R- and ADR/ADX-catalyzed reactions (Appendix A, Table A1) well correlate with their E^1_7 values (Appendix A, Equation (A1)). The calculated E^1_7 values of ArNO_2 ($E^1_{7(\text{calc.})}$) obtained using

this equation are given in Table 1. These values could be realistic because the $E^1_{7(\text{calc.})}$ of NSC697923 is similar to those of other nitrofurans, and the $E^1_{7(\text{calc.})}$ value of CDNB is higher than that of *m*-dinitrobenzene due to the electron-accepting character of the chlorine substituent (Appendix A, Table A1). In turn, the $E^1_{7(\text{calc.})}$ value of Tri-1 (Table 1) is significantly lower than that of *p*-nitropyridine, -0.19 V [34]. This is because of its *m*-nitropyridine structure and the electron-donating character of the methoxy group.

Flavoenzyme NAD(P)H:quinone oxidoreductase (NQO1) reduces quinones in a two-electron way, with k_{cat} in certain cases being above 1000 s^{-1} [35]. However, the reduction in ArNO_2 with the formation of ArNHOH is 10^2 – 10^5 times slower than that of quinones [36] due to insufficiently defined reasons. The rate constants of NQO1-catalyzed reduction of nitroaromatics were calculated from the rate of NADPH oxidation monitored at 340 nm. To account for possible changes in ArNO_2 absorbance at 340 nm occurring during reduction, control experiments were conducted using the NADPH regeneration system, glucose-6-phosphate, and glucose-6-phosphate dehydrogenase. However, these changes amounted to no more than 10% of the total absorbance changes at 340 nm. One may note that the reactivity of the examined compounds is low (Table 1). For comparison, one of the fastest nitroaromatic substrates of NQO1, tetryl, is characterized by $k_{\text{cat}} = 73$ s^{-1} and $k_{\text{cat}}/K_m = 2.6 \times 10^5$ $\text{M}^{-1}\text{s}^{-1}$ [36].

Another relevant problem is the possible action of tested nitroaromatics as ‘subversive substrates’ for TrxRs, where their reduction into $\text{ArNO}_2^- \cdot$ may lead to toxic effects [21]. We also investigated the reduction in these compounds by the structurally and functionally related antioxidant flavoenzyme human glutathione reductase (HGR) [19]. Among ArNO_2 , tetryl was the most efficient oxidant of mammalian TrxRs, with a k_{cat} of 1.8 s^{-1} (rat cytosolic enzyme (TrxR1) [21]), 2.9 s^{-1} (human TrxR1), and 0.7 s^{-1} (human mitochondrial enzyme (TrxR2)) [37], which is about 9% of the k_{cat} of DTNB reduction and of HGR, with $k_{\text{cat}} \geq 5$ s^{-1} and $k_{\text{cat}}/K_m = 2.0 \times 10^3$ $\text{M}^{-1}\text{s}^{-1}$ [38]. Purified human TrxR2 and commercially available rat TrxR1 preparations used in this study possessed NADPH:oxidase activities of 0.02 s^{-1} and 0.01 μmol NADPH oxidized $\cdot\text{min}^{-1} \cdot\text{mg}$ protein, respectively. The presence of 100 μM Stattic, Tri-1, or CDNB, or 70 μM BTB06584 or NSC697923 increased the NADPH:oxidase activity of TrxRs by 2–2.5 times, while 100 μM tetryl increased it by 12–14 times. In reactions with HGR, the same concentrations of Stattic, Tri-1, CDNB, or BTB06584 increased its NADPH:oxidase activity from 0.04 s^{-1} only to 0.08 – 0.09 s^{-1} . The activity of NSC697923 was higher, with $k_{\text{cat}} \geq 0.35$ s^{-1} and $k_{\text{cat}}/K_m = 3.0 \pm 0.4 \times 10^3$ $\text{M}^{-1}\text{s}^{-1}$. The reduction rate of 50 μM cytochrome *c* added into the reaction mixture was 60% of the NADPH oxidation rate, i.e., the single-electron flux during NSC697923 reduction was 30% [21,38]. Thus, our data show that the examined compounds are very slow ‘subversive substrates’ for TrxRs and HGR, with several times lower reactivity than tetryl.

2.2. Reactions of Nitroaromatic Compounds with Reduced Glutathione

Nitroaromatic sulfones react with reduced glutathione (GSH) (Equation (2)) [39] and other cellular thiols:



They inactivate reduced TrxR in a similar reaction, reacting predominantly with catalytic selenol [23]. On the other hand, the reaction with GSH may be considered a pathway to their detoxification. The pseudo-first-order reaction rate constants of the examined nitroaromatic sulfones (Figure 1) were directly proportional to GSH concentration (2.0 – 10.0 mM). The calculated second-order rate constants decreased in the order NSC697923 (7.2 ± 0.3 $\text{M}^{-1}\text{s}^{-1}$), Tri-1 (4.8 ± 0.3 $\text{M}^{-1}\text{s}^{-1}$), and Stattic (1.1 ± 0.1 $\text{M}^{-1}\text{s}^{-1}$). BTB06584 was found to be relatively unstable, with its λ_{max} gradually shifting from 280 nm to 316 nm with $t_{1/2} \sim 1.5$ h at pH 7.0 and 37 $^\circ\text{C}$. Therefore, the rate constant of its reaction with GSH was estimated to be only approximately ~ 0.5 $\text{M}^{-1}\text{s}^{-1}$ at 25 $^\circ\text{C}$. For comparison, the rate constants of the reaction of GSH with tetryl and CDNB under the same conditions are 1.2 $\text{M}^{-1}\text{s}^{-1}$ and 0.03 $\text{M}^{-1}\text{s}^{-1}$, respectively [20,21].

2.3. Cytotoxicity of Nitroaromatic Compounds

By studying a series of ArNO₂ without alkylating or bioelectrochemically activated alkylating groups, we found that their concentration causing 50% MH22a cell death (cL₅₀) or concentration causing 50% growth inhibition of HCT-116 cells (GI₅₀) is described by a two-parameter regression similar to that presented in Equation (1) [31,40]. After supplementing these dependencies with new data, their final expression is given in Equations (A2) and (A3) of Appendix B. The cL₅₀ and GI₅₀ of nitroaromatic sulfones and 1-chloro-2,4-dinitrobenzene determined in this work are presented in Table 2.

Table 2. Concentrations of nitroaromatic compounds causing 50% MH22a cell death (cL₅₀) and 50% growth inhibition of HCT-116 cells (GI₅₀), their calculated single-electron reduction potentials ($E^1_{7(\text{calc.})}$), and octanol/water partition coefficients at pH 7.0 (log *D*). The values of cL₅₀ or GI₅₀ predicted according to Equations (A2) or (A3) (Appendix B) are given in parentheses.

Compound	$E^1_{7(\text{calc.})}$ (V)	log <i>D</i>	cL ₅₀ MH22a (μM)	GI ₅₀ HCT-116 (μM)
CDNB	−0.285	2.46	1.9 ± 0.1 (28.3)	5.0 ± 0.3 (40.2)
NSC697923	−0.287	2.70	1.0 ± 0.1 (25.1)	1.0 ± 0.1 (38.3)
Stattic	−0.304	1.12	1.8 ± 0.2 (100)	2.0 ± 0.2 (106)
BTB06584	−0.326	5.13	28.0 ± 4.0 (10.5)	80.0 ± 9.0 (36)
Tri-1	−0.365	3.29	6.6 ± 0.5 (77.6)	7.0 ± 0.7 (184)

The data in Figure 2A,B show that Tri-1, Stattic, NSC697923, and 1-chloro-2,4-dinitrobenzene exhibit significantly greater activity than would be expected from their $E^1_{7(\text{calc.})}$ and log *D*. However, the increase in cytotoxicity is not characteristic of BTB06584, nor of another irreversible inhibitor of TrxR, tetryl (Figure 2A,B).

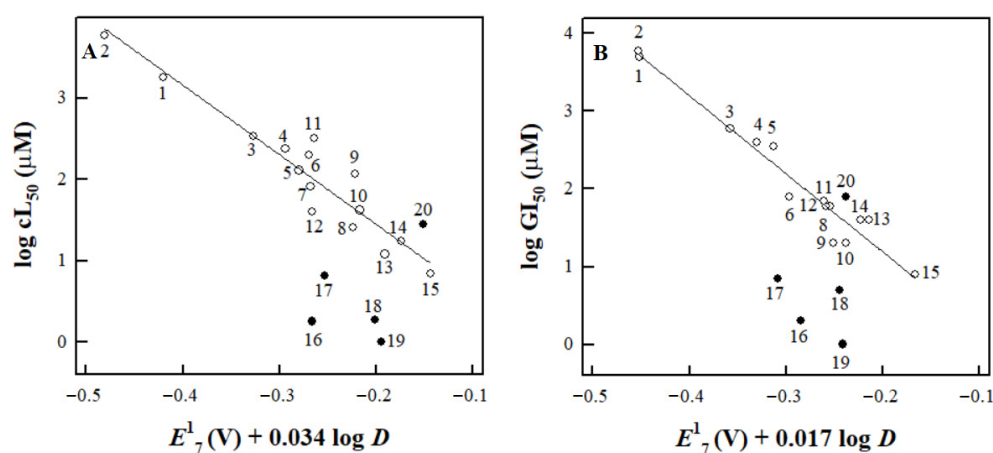


Figure 2. The dependence of the cL₅₀ of nitroaromatic compounds against MH22a cells (A) and their GI₅₀ against HCT-116 cells (B) on their E^1_7 and log *D* as described by Equations (A2) and (A3) (Appendix B). The correlation lines are drawn according to these equations for compounds 1–15 (Table A2, Appendix B). The compounds examined in this study are tetryl (15), Stattic (16), Tri-1 (17), CDNB (18), NSC697923 (19), and BTB06584 (20).

Table 2 also shows their expected cL₅₀ and GI₅₀ values calculated from Equations (A2) and (A3) (Appendix B). One may note that the GI₅₀ of Tri-1 in HCT-116 cells (Table 2) is comparable to the value previously determined for the same cells at 48 h, 2.9 μM [23].

The cytotoxicity of nitroaromatics in MH22a cells was decreased by desferrioxamine and the antioxidant *N,N'*-diphenyl-*p*-phenylene diamine (DPPD) (Table 3). Concerning the other enzymatic mechanisms, we examined the effects of an inhibitor of NQO1, dicoumarol, and several inhibitors of cytochromes P-450 on the cytotoxicity of ArNO₂ [31,40] (Table 3). Dicoumarol decreased the cytotoxicity of the compounds except for tetryl, and cytochrome P-450 inhibitors did so in most cases, except for the increase in toxicity of Stattic in the

presence of α -naphthoflavone and isoniazid and the increase in toxicity of tetryl in the presence of miconazole (Table 3). Because of the instability of BTB06584 at pH 7.0 and 37 °C, further cytotoxicity studies were not performed.

Table 3. Modulation of cytotoxicity of nitroaromatic compounds in MH22a cells by antioxidants, dicoumarol, and inhibitors of cytochromes P-450, $n = 3$, $p < 0.05$ *, $p < 0.02$ **, $p < 0.005$ *** with respect to cell viability in the absence of additions. The indicated concentrations of the above compounds did not affect cell viability by more than $\pm 2\%$. The cell viability data are adjusted to these changes.

Compound	Cell Viability (%)						
	Additions:						
	None	DPPD (2.0 μ M)	Desferri- Oxamine (1.0 mM)	Dicoumarol (20 μ M)	α -Naphtho- Flavone (5.0 μ M)	Isoniazid (1.0 mM)	Miconazole (5.0 μ M)
1-Chloro-2,4-dinitrobenzene (2.0 μ M)	49.3 \pm 4.2	77.3 \pm 5.6 ***	67.0 \pm 4.6 **	69.5 \pm 4.8 **	63.3 \pm 3.8 *	64.9 \pm 4.8 *	74.9 \pm 7.7 **
NSC697923 (1.0 μ M)	45.1 \pm 3.5	55.7 \pm 5.2	61.7 \pm 4.4 **	63.1 \pm 5.0 **	69.0 \pm 6.4 **	71.0 \pm 5.5 ***	71.0 \pm 5.3 ***
Stattic (2.0 μ M)	50.3 \pm 5.5	79.1 \pm 6.6 **	75.0 \pm 3.1 **	76.7 \pm 10 *	38.6 \pm 4.8 *	32.6 \pm 2.8 ***	74.5 \pm 10.7 *
Tri-1 (6.0 μ M)	49.9 \pm 4.5	67.7 \pm 4.6 **	64.7 \pm 4.3 *	78.3 \pm 4.8 ***	70.5 \pm 4.6 **	77.0 \pm 4.8 ***	68.6 \pm 3.3 **
Tetryl (10.0 μ M)	45.5 \pm 4.2	78.4 \pm 5.8 ***	79.9 \pm 5.0 ***	28.2 \pm 2.8 ***	55.4 \pm 5.0	54.4 \pm 3.6	24.2 \pm 1.1 ***

2.4. Inhibition of Thioredoxin Reductase and Glutathione Reductase by Nitroaromatic Compounds

In most previous studies, the efficiency of TrxR inhibition by ArNO₂ was evaluated by the decrease in the activity of the enzyme after incubation of its NADPH-reduced form with the compound for a certain time [20–23]. However, this does not allow for a separate assessment of their reversible inhibition, which is independent of time, and irreversible inhibition, which usually occurs using covalent modification and is time-dependent. In our initial experiments, we used the lysates of MH22a and HCT-116 cells, in which the activity of TrxR was 56.2 \pm 3.2 and 42.9 \pm 3.0 nmol DTNB reduced \cdot min⁻¹ \cdot mg protein, respectively. The activity of GR was 302 \pm 18 and 100 \pm 7.0 nmol NADPH oxidized \cdot min⁻¹ \cdot mg protein, respectively.

First, we investigated the effects of ArNO₂ on the enzyme activity by introducing them immediately into the reaction mixture ($t = 0$). In the second case, we incubated the lysate with NADPH and tested the compound for 20 min, which was close to the conditions of previous studies [20–23]. The concentration of compounds used was 10 μ M, which was several times higher than the cL₅₀ or GI₅₀ of the most toxic compounds, CDNB, Tri-1, and NSC697923 (Table 2). It can be seen that at this compound concentration, the residual activity of TrxR in the presence of Tri-1 and NSC697923 is very small, both at $t = 0$ and $t = 20$ min (Figure 3A). However, a more pronounced time-dependent inhibition of GR was observed only under the action of Stattic, while in the cases of CDNB, Tri-1, and SN697923, it was less pronounced and almost absent in the case of tetryl (Figure 3B). It should be noted that experiments with all tested compounds in both cell lysates gave very similar results when comparing the relative inhibition of the reaction rate. Therefore, in Figure 3, we present only one case of TrxR and HGR inhibition by each compound.

Next, we investigated the inhibitory effects of ArNO₂ on the preparation of rat TrxR1 and purified HGR (Table 4). This enabled us to quantitatively separate the effects of reversible and irreversible inhibition. Our data demonstrate that NSC697923 and Tri-1 reversibly inhibit TrxR1 at micromolar concentrations and further rapidly inactivate it (Table 4). On the other hand, while Stattic, CDNB, and tetryl reversibly inhibit TrxR1 at higher concentrations, they caused its rapid inactivation, with the activity of tetryl exceeding that of CDNB (Table 4). This is in line with the results of previous observations [21,23]. It should be noted that Stattic rapidly inactivates HGR, while Tri-1, tetryl, and CDNB are almost inactive (Table 4), which is again in line with the previous findings [21,24,38].

Because of the instability of BTB06584, further studies of its inhibitory properties were not carried out. Taken together, the effects of the studied nitroaromatics on the activity of isolated TrxR1 and HGR (Table 4) and their activity in the cell lysates (Figure 3) closely match each other.

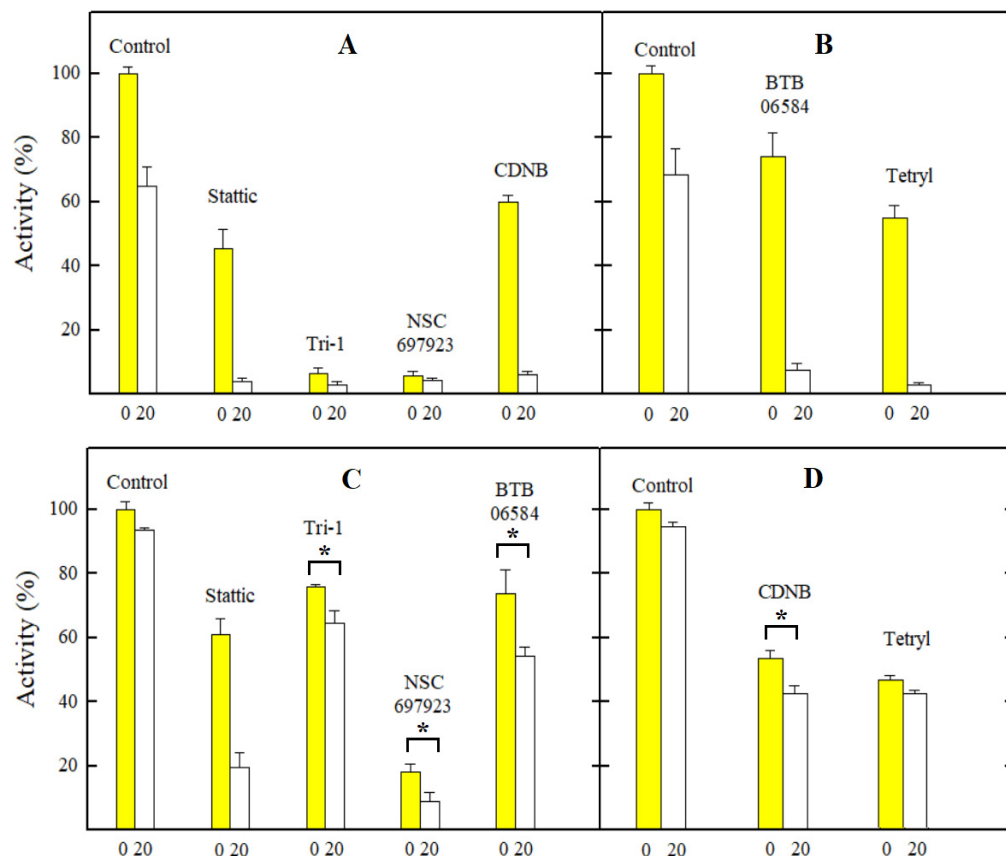


Figure 3. The changes in the activity of TrxR (A,B) and GR (C,D) in the lysates of MH22a cells (A,C) and HCT-116 cells (B,D) under the action of the examined nitroaromatic compounds. The numbers on the abscissas indicate the minutes of lysate incubation time with NADPH in the presence or absence of the compound. The asterisks (*) indicate a statistically significant difference with $p \leq 0.05$. In all other cases except the inactivation of GR in MH22a cell lysates (C) and the action of tetryl on GR in HCT-116 cell lysates (D), the differences between $t = 0$ and $t = 20$ min are characterized by $p = 0.01$ – 0.001 .

Table 4. Concentrations of compounds cause a 50% decrease in the initial rate of TrxR1- or HGR-catalyzed reactions (IC_{50}) and the rate constants of enzyme inactivation (k_i) at pH 7.0 and 25 °C. The concentrations of compounds used in inactivation experiments are given in parentheses.

Compound	Enzyme			
	Rat TrxR1		HGR	
	IC_{50} (μ M)	k_i (min^{-1})	IC_{50} (μ M)	k_i (min^{-1})
1-Chloro-2,4-dinitrobenzene	25 ± 5.0	0.10 ± 0.01 (10 μ M)	40 ± 6.0	≤ 0.005 (10 μ M)
NSC697923	1.1 ± 0.1	0.12 ± 0.02 (1.0 μ M)	0.5 ± 0.1	0.02 ± 0.003 (1.0 μ M)
Stattic	15 ± 2.0	0.14 ± 0.02 (10 μ M)	14.0 ± 1.0	0.02 ± 0.003 (10 μ M)
Tri-1	2.0 ± 0.3	0.12 ± 0.01 (1.0 μ M)	32.0 ± 5.0	≤ 0.005 (10 μ M)
Tetryl	10 ± 1.3	0.04 ± 0.01 (1.0 μ M)	14 ± 2.0	≤ 0.002 (10 μ M)

3. Discussion

In this study, for the first time, we obtained reliable $E^1_{7(\text{calc.})}$ values for several nitroaromatic compounds that were known or identified as irreversible inhibitors of TrxR (Figure 1, Table 1). This allowed us to quantitatively compare their cytotoxicity with that of model ArNO_2 . Their prooxidant cytotoxicity was demonstrated by the protective effects of desferrioxamine and DPPD (Table 3). Indeed, four of them, CDNB, NSC697923, Stattic, and Tri-1, were more cytotoxic in MH22a and HCT-116 cells than may be expected from their redox cycling activity and lipophilicity (Equations (A2) and (A3) (Appendix B), Table 2, Figure 2). Thus, it is possible to attribute this effect to their efficient irreversible inhibition of TrxR (Figure 3, Table 4). It can be noted that there is a certain parallelism between the rates of TrxR inactivation by these compounds (k_i , Table 4) and their reactivity with GSH (Section 2.2). The data in Table 3 point to some additional mechanisms of action of the examined compounds: (i) Like other ArNO_2 , they react with cytochromes P-450 [11,12,31]. However, the mechanisms and roles of individual cytochromes P-450 remain to be elucidated. Furthermore, these reactions have different effects on their cytotoxicity. This complements the data on the observed transformation of Tri-1 in microsomes [23], and (ii) except for tetryl, these compounds are also activated by NQO1 (Table 3), most likely due to the formation of alkylating ArNHOH [9]. Moreover, no connection was observed between their activity as TrxR 'subversive substrates' and cytotoxicity. In our opinion, the role of these reactions in the cytotoxicity of the above compounds is negligible because the most active 'subversive substrate' of TrxR, tetryl, does not possess enhanced cytotoxicity. We have to mention separately that a novel efficient irreversible inhibitor of TrxR, NSC697923 (Figure 3, Table 4), was identified in this work. This compound also possessed the highest cytotoxicity among the examined compounds (Figure 2). This compound may have further application prospects due to its demonstrated antitumor and antiviral activity, including the inhibition of the growth of implanted human tumors without causing toxic effects in mice [26,41,42].

On the other hand, BTB06584 and tetryl efficiently inhibited TrxR in cell lysates in short-term experiments (Figure 3) but did not display enhanced cytotoxicity (Figure 2). This can be explained by the instability of BTB06584, which may affect the results of long-term cytotoxicity experiments. As for tetryl, the absence of its enhanced cytotoxicity has also been observed in both cancerous and normal cell lines [28,43]. It is important to note that although tetryl more rapidly than CDNB irreversibly inhibits isolated TrxR (Table 4), it was less effective than CDNB in inhibiting TrxR in the cells [21]. The available data on the TrxR inhibition in the cells by the compounds examined in this study are summarized in Table 5.

Table 5. The summary of the data on the TrxR and GR inhibition during the incubation of the cells with the irreversible inhibitors of TrxR.

Compound	Cells	Compound Concentration, Incubation Time	Residual Activity (%)	
			TrxR	GR
Tri-1	HCT-116 [23]	3.3 μM , 3 h	20	n.d.
	BF16-F10 [44]	2.0 μM , 3 h	50	n.d.
		20 μM , 3 h	10	n.d.
Stattic	A549 [22]	10 μM , 4 h	25	n.d.
	Various human cervical carcinoma cells [24]	20 μM , 0.5 h	n.d.	30–50
1-Chloro-2,4- dinitrobenzene	A549 [21]	50 μM , 4 h	30	80
	HeLa [21]	50 μM , 4 h	30	100
Tetryl	A549 [21]	50 μM , 4 h	80	100
	HeLa [21]	50 μM , 4 h	75	100

Therefore, it can be assumed that the inhibitory effect of tetryl becomes less pronounced in long-term cytotoxicity experiments. A possible reason for this phenomenon is that the enzymatic single-electron reduction and redox cycling of tetryl, especially its NQO1-catalyzed single- and two-electron reduction, produce its less toxic metabolite, *N*-methylpicramide. This metabolite does not react with TrxR [36]. In favor of this argument is the fact that, unlike in the cases of other ArNO₂, the NQO1 inhibitor dicoumarol increases but does not decrease the cytotoxicity of tetryl (Table 3). The analogous data were obtained in other cell lines [30].

There are a couple of other issues that need to be discussed regarding the inhibition of TrxR by both ArNO₂ and other types of compounds, which may be taken as directions for further research. First, this is a characterization of the reversible inhibition of TrxR and its possible role in the cytotoxicity of inhibitors. Although most studies concerned the irreversible inhibition of enzymes [20–23], reversible inhibition of TrxR by ArNO₂ was also demonstrated, which can be competitive or noncompetitive with respect to DTNB [21,45]. In the first case, this indicates that the inhibitor binds to the catalytic selenocysteine. However, the analysis of these data was complicated by the rapid inactivation of the enzyme due to its covalent modification by the inhibitor [21]. In the second case, this suggests that the inhibitor binds at a distinct site, most likely in the intersubunit domain. This domain is structurally close to the analogous HGR domain, according to crystallographic studies [46]. Our preliminary data obtained at saturating concentrations of NADPH and DTNB suggest that this type of inhibition may also be characteristic of TrxR, occurring even at micromolar concentrations of NSC697923 and Tri-1 (Table 4). The role of this phenomenon is almost unexplored, except for the data on the contribution of TrxR non-competitive inhibition by *N*-(4-chlorophenyl)-5-nitrofuranyl-2-carboxamide (LCS3) to its anticancer in vitro activity [45]. Analogously, it was found that the antiparasitic in vitro activity of a series of ArNO₂ was partly determined by their noncompetitive inhibition of the structurally related enzyme, *Plasmodium falciparum* GR [47]. Taken together, these data provide some new guidelines for the search for TrxR inhibitors with cytotoxic/anticancer activity, including studies of mutants of its active center residues [48].

The second issue is the concept of dual targeting of the glutathione and thioredoxin antioxidant systems because of their interconnection and compensatory nature, which has recently gained attention in cancer chemotherapy ([45,49] and references therein). It is suggested that the uncompetitive reversible inhibition of both TrxR and GR by nitrofuranyl LCS3 causes synergistic effects that enhance cell death [45]. In this aspect, one may note that the dual inhibition of TrxR and GR by Stattic is well documented [22,24] and supported by the results of the current study (Figure 3, Table 4). On the other hand, a newly identified compound, NSC697923, is more active than Stattic in this respect (Figure 3 and Table 4) and deserves more thorough studies.

4. Materials and Methods

4.1. Enzymes and Chemicals

Recombinant rat P-450R, bovine ADR, and ADX were prepared as described in [50]; their concentrations were determined according to $\epsilon_{456} = 21.4 \text{ mM}^{-1} \cdot \text{cm}^{-1}$, $\epsilon_{450} = 11.0 \text{ mM}^{-1} \cdot \text{cm}^{-1}$, and $\epsilon_{414} = 10.0 \text{ mM}^{-1} \cdot \text{cm}^{-1}$, respectively. They were a generous gift from Dr. Alexey Yantsevich (Institute of Bioorganic Chemistry, BNAS, Minsk, Belarus). Recombinant HGR was prepared as previously described [51]; its concentration was determined according to $\epsilon_{463} = 11.3 \text{ mM}^{-1} \cdot \text{cm}^{-1}$. It was a generous gift from Dr. Elisabeth Davioud-Charvet (Universite de Strasbourg, Strasbourg, France). Recombinant human mitochondrial thioredoxin reductase (TrxR2) was prepared as described in [52], and its concentration was determined according to $\epsilon_{463} = 11.3 \text{ mM}^{-1} \cdot \text{cm}^{-1}$. It was a generous gift from Professor Elias Arner (Karolinska Institutet, Stockholm, Sweden). Tetryl was synthesized as described in [30]; it was a generous gift from Dr. Jonas Šarlauskas (Institute of Biochemistry, Vilnius, Lithuania). NQO1 was prepared from rat liver according to Prochaska [53]; its concentration was determined according to $\epsilon_{460} = 11.0 \text{ mM}^{-1} \cdot \text{cm}^{-1}$.

2-(4-Chlorophenyl)sulfonyl-6-methoxy-3-nitropyridine (Tri-1), 6-nitro-1-benzothiophene 1,1-dioxide (Stattic), 2-[(4-methylphenyl)sulfonyl]-5-nitrofuran (NSC697923) and 2-nitro-5-(phenylsulfonyl)phenyl-4-chlorobenzoate (BTB06548) were obtained from Selleck Chemicals (Houston, TX, USA) and used as received. Rat cytosolic TrxR1 (110 U/mg), NADPH, and other reagents were obtained from Sigma-Aldrich (St. Louis, MO, USA) and used as received.

4.2. Enzymatic Assays and Chemical Reactions

The kinetic measurements were carried out spectrophotometrically using a Perkin Elmer Lambda 25 spectrophotometer (PerkinElmer, Waltham, MA, USA) in 0.1 M K-phosphate buffer (pH 7.0) containing 1 mM EDTA at 25 °C. The activities of P-450R and ADR/ADX were determined according to the reduction rate of 50 μM cytochrome *c* ($\Delta\epsilon_{550} = 20 \text{ mM}^{-1}\cdot\text{cm}^{-1}$) at substrate concentrations indicated below. They were close to those reported previously [31,40]: 37 s^{-1} (P-450R, [NADPH] = 100 μM), 7.8 s^{-1} (ADR, [ADX] = 0.5 μM , [NADPH] = 50 μM), and 1750 s^{-1} (NQO1, [NADPH] = 150 μM , [menadione] = 10 μM). In this case, 0.01% Tween 20 and 0.25 mg/mL bovine serum albumin were added as NQO1 activators. The activity of HGR, determined according to the initial oxidation rate of 200 μM NADPH ($\Delta\epsilon_{340} = 6.2 \text{ mM}^{-1}\cdot\text{cm}^{-1}$) in the presence of 1.0 mM GSSG, was equal to 170 s^{-1} . The activity of TrxR2, determined according to the reduction rate of 2.0 mM DTNB ($\Delta\epsilon_{412} = 27.2 \text{ mM}^{-1}\cdot\text{cm}^{-1}$) in the presence of 200 μM NADPH, was close to that reported previously, 7.3 s^{-1} [37]. The activity of rat TrxR1, determined under the same conditions, was equal to 3.64 $\mu\text{mol DTNB reduced}\cdot\text{min}^{-1}\cdot\text{mg protein}^{-1}$.

The initial rates of enzymatic NADPH-dependent ArNO_2 reduction were determined according to $\Delta\epsilon_{340} = 6.2 \text{ mM}^{-1}\cdot\text{cm}^{-1}$ after the subtraction of intrinsic NADPH oxidase activities of enzymes, 0.06 s^{-1} (P-450R), 0.1 s^{-1} (NQO1), 0.13 s^{-1} (ADR + 0.5 μM ADX), 0.04 s^{-1} (HGR), and 0.02 s^{-1} (TrxR2). The stock solutions of oxidants were prepared in DMSO (dilution factor 100). The values of turnover rate, k_{cat} , reflect the maximal number of moles of NADPH oxidized or oxidant reduced per mole of the enzyme active center per second at a saturating concentration of substrates. Additionally, k_{cat}/K_m reflects the bimolecular rate constant (or catalytic efficiency constant) and corresponds to the inverse intercepts and slopes in Lineweaver–Burk coordinates, $[E]/v$ vs. $1/[\text{oxidant}]$. These rate constants were obtained by fitting the experimental data to the parabolic expression using SigmaPlot 2000 (version 11.0, Systat Software, San Jose, CA, USA). In some experiments, as noted in the main text, the NADPH regeneration system (10 mM glucose-6-phosphate and 3 $\mu\text{g/mL}$ glucose-6-phosphate dehydrogenase) was used.

In the study of reversible inhibition of TrxR1 or HGR ($t = 0$), ArNO_2 was introduced into the reaction mixture (concentrations of NADPH, DTNB, or GSSG were as mentioned above). The reaction was started by the introduction of the enzyme. The concentration of ArNO_2 that decreased the reaction rate by 50% (IC_{50}) was calculated in coordinates $1/v$ vs. $[\text{inhibitor}]$. Irreversible (time-dependent) inhibition of TrxR or HGR was tested by incubating the enzymes with 200 μM NADPH and a fixed concentration of ArNO_2 . After incubation, the reaction was started by the introduction of DTNB or GSSG. The pseudo-first-order inactivation rate constant (k_i) was calculated in the coordinates $\ln v$ vs. incubation time.

The reactions of GSH (2.0–10.0 mM) with 50–100 μM nitroaromatic sulfones were studied spectrophotometrically at pH 7.0 and 25 °C. After the addition of GSH, the absorbance rise at 366 nm (NSC697923) or 367 nm (Tri-1), or its decrease at 315 nm (Stattic) or 280 nm (BTB06548), was monitored. The pseudo-first-order reaction rate constants were calculated according to a method by Guggenheim [54].

4.3. Cytotoxicity Assays

Murine hepatoma MH22a cells obtained from the Institute of Cytology of the Russian Academy of Sciences (St. Petersburg, Russia) were grown and maintained at 37 °C in DMEM medium supplemented with 10% fetal bovine serum, 100 U/mL penicillin,

and 0.1 mg/mL streptomycin, as described in [31,40]. In the cytotoxicity experiments, 3.0×10^4 /mL cells were seeded on glass slides in 5 mL flasks, either in the presence or absence of compounds, and were grown for 24 h. In the absence of compounds, cells reached 40–50% confluence. Then, the slides were rinsed 3–4 times with phosphate-buffered saline and stained with Trypan blue. The cells adherent to the slides were counted under a light microscope. Typically, they did not accumulate Trypan blue, and their viability was 98.5–99.3%. Human colon adenocarcinoma cells HCT-116 obtained from ATCC (Manassas, VA, USA) were grown and maintained at 37 °C in 5% CO₂ in RPMI 1640 DMEM medium, supplemented with 10% fetal bovine serum, 2 mM L-glutamine, and 0.05 mg/mL gentamycin. In the cytotoxicity experiments, 1.0×10^5 /mL cells were seeded in the absence or presence of compounds and were grown for 48 h. In the absence of compounds, cells reached 65–75% confluence. Their viability was determined by staining with crystal violet [55]. Stock solutions of compounds were prepared in DMSO. Its concentration in cultivation media did not exceed 0.2% and did not affect cell viability. The experiments were conducted in triplicate.

4.4. Studies of Thioredoxin Reductase and Glutathione Reductase Activity in Cell Lysates

For the enzymatic analysis, MH22a and HCT-116 cells were grown until confluence, detached by trypsinization, twice washed with PBS, and sonicated on ice in four cycles of 20 s. The homogenate was centrifuged at $14,000 \times g$ for 45 min, and the resulting supernatant with added 1.0 mM PMSF was used for enzymatic analysis. Protein concentration was determined according to the Bradford method. The activity measurements were performed in 0.1 M K-phosphate buffer (pH 7.0) containing 1 mM EDTA at 37 °C, with a final protein concentration of $80 \mu\text{g}\cdot\text{mL}^{-1}$. The activity of TrxR was determined according to the reduction rate of 2.0 mM DTNB in the presence of 200 μM NADPH, as described in [56]. In this case, the activity is expressed as the difference between the reaction rates before and after the sample incubation with NADPH and 2.0 μM auranofin for 20 min. The initial rates were corrected for the nonenzymatic reduction rates of DTNB by the low m.w. thiols present in the sample. Typically, the treatment with auranofin suppressed the rate of DTNB reduction by ~95%. The activity of GR was determined according to the oxidation rate of 200 μM NADPH by 1.0 mM GSSG, monitored at 340 nm. Studying the effects of ArNO₂ on the activity of TrxR and GR, the reaction rates were recorded as follows: (a) In the absence of compound; (b) Immediately after the addition of compound; (c) After the protein incubation in the presence of NADPH for 20 min; and (d) After the protein incubation in the presence of NADPH and compound for 20 min.

4.5. Statistical Analysis and Calculations

The statistical analysis was performed using Statistica (version 4.3, Statsoft, Toronto, ON, Canada). Octanol/water distribution coefficients at pH 7.0 (log *D*) were calculated using the Log *D* Predictor (<https://chemaxon.com> (accessed on 23 May 2022)).

5. Conclusions

The studies of enzymatic single-electron reduction in known or identified in this work nitroaromatic inhibitors of TrxR and the calculation of their $E^1_{7(\text{calc.})}$ enabled us to quantitatively compare their cytotoxicity with that of model redox cycling ArNO₂. This made it possible to determine whether their cytotoxicity could be linked to TrxR inhibition or other factors. We also identified NSC697923 as a novel, potent inhibitor of TrxR, which also inhibits HGR. Our data may be instrumental in the search for nitroaromatic TrxR inhibitors with enhanced cytotoxic/anticancer activity. Future studies may be directed at evaluating the role of reversible TrxR inhibition, possible synergistic effects of TrxR and GR inhibition, and the influence of NQO1 and cytochromes P-450 on the activity of inhibitors.

Author Contributions: A.N.-Č. and V.J. performed cell culture and cytotoxicity studies; L.M. and A.M. performed enzymatic assays; N.Č. planned and supervised the experiments and wrote the final version of the manuscript. All authors have read and agreed to the published version of the manuscript.

Funding: This work was supported by the European Social Fund (Measure No. 09.33-LMT-K-712, grant No. DOTSUT-43/09.3.3.-LMT-K71201-0058/LSS-600000-58).

Institutional Review Board Statement: Not applicable.

Informed Consent Statement: Not applicable.

Data Availability Statement: The data could be available from the corresponding author upon reasonable request.

Acknowledgments: We thank Alexey Yantsevich (Institute of Bioorganic Chemistry, BNAS, Minsk, Belarus) for a generous gift of recombinant rat P-450R, bovine ADR, and ADX; Elisabeth Davioud-Charvet (Universite de Strasbourg, Strasbourg, France) for a generous gift of human GR; Elias Arner (Karolinska Institutet, Stockholm, Sweden) for a generous gift of human TrxR2; Jonas Šarlauskas (Institute of Biochemistry, Vilnius, Lithuania) for his generous gift of tetryl; Benjaminas Valiauga and Mindaugas Lesanavičius (Institute of Biochemistry, Vilnius, Lithuania) for their assistance in the manuscript preparation.

Conflicts of Interest: The authors declare no conflict of interest.

Appendix A

Table A1 contains the previously determined logarithms of geometric averages of k_{cat}/K_m of model ArNO₂ in P-450R- and ADR/ADX-catalyzed reactions ($\log k_{\text{cat}}/K_m$ (avge) = 0.5 $\log k_{\text{cat}}/K_m$ (P-450R) + 0.5 $\log k_{\text{cat}}/K_m$ (ADR/ADX)) [31,40], supplemented by the repeated studies of some previously studied compounds. For quantitative analysis, when available, data obtained in the current work were used.

Table A1. Single-electron reduction midpoint potentials of nitroaromatic compounds (E^{1_7}), their bimolecular reduction rate constants (k_{cat}/K_m) by NADPH:cytochrome P-450 reductase (P-450R) and adrenodoxin reductase/adrenodoxin (ADR/ADX), and their geometric averages ($\log k_{\text{cat}}/K_m$ (avge)). Data were taken from [29,38]. The values obtained in the current work are given in parentheses.

No.	Compound	E^{1_7} (V) ^a	k_{cat}/K_m (M ⁻¹ s ⁻¹)		$\log k_{\text{cat}}/K_m$ (avge)
			P-450R	ADR/ADX	
1	Nitrobenzene	−0.485	$6.8 \pm 0.8 \times 10^2$	$3.4 \pm 0.2 \times 10^3$	3.18
2	4-Nitrobenzoic acid	−0.425	$2.3 \pm 0.2 \times 10^3$ ($2.9 \pm 0.2 \times 10^3$)	$2.0 \pm 0.2 \times 10^3$ ($2.3 \pm 0.2 \times 10^3$)	3.33 (3.41)
3	2-Nitrothiophene	−0.390	$1.4 \pm 0.1 \times 10^4$	$4.2 \pm 0.3 \times 10^4$	4.38
4	4-Nitroacetophenone	−0.355	$1.7 \pm 0.2 \times 10^4$	$3.2 \pm 0.3 \times 10^4$	4.37
5	1,3-Dinitrobenzene	−0.345	$4.9 \pm 0.2 \times 10^4$	$5.2 \pm 0.4 \times 10^4$	4.70
6	4-Nitrobenzaldehyde	−0.325	$3.3 \pm 0.2 \times 10^4$	$1.7 \pm 0.3 \times 10^5$	4.87
7	2-Nitrothiophene-5-carboxymorpholide	−0.305	$1.4 \pm 0.2 \times 10^5$	$4.1 \pm 0.6 \times 10^5$	5.38
8	1,2-Dinitrobenzene	−0.287	$1.6 \pm 0.1 \times 10^5$	$1.8 \pm 0.2 \times 10^5$	5.23
9	2-Nitrothiophene-5-aldoxime	−0.280	$2.2 \pm 0.2 \times 10^6$ ($1.8 \pm 0.2 \times 10^6$)	$5.4 \pm 0.5 \times 10^5$ ($4.2 \pm 0.4 \times 10^5$)	6.04 (5.94)
10	2-Nitrothiophene-5-aldehyde	−0.260	$2.8 \pm 0.1 \times 10^5$	$4.0 \pm 0.5 \times 10^5$	5.52
11	Nitrofurantoin	−0.255	$9.1 \pm 1.4 \times 10^4$	$1.0 \pm 0.2 \times 10^6$	5.48
12	Nifuroxime	−0.255	$1.1 \pm 0.1 \times 10^5$	$1.0 \pm 0.1 \times 10^6$	5.52
13	1,4-Dinitrobenzene	−0.255	$1.2 \pm 0.1 \times 10^6$	$2.0 \pm 0.2 \times 10^6$	6.19
14	2,4,6-Trinitrotoluene	−0.253	$1.0 \pm 0.1 \times 10^5$ ($1.4 \pm 0.1 \times 10^5$)	$7.3 \pm 0.2 \times 10^5$ ($7.0 \pm 0.2 \times 10^5$)	5.43 (5.50)
15	Tetryl	−0.191	$5.9 \pm 0.2 \times 10^6$	$8.9 \pm 1.0 \times 10^5$	6.36

^a From Refs. [13,34,57].

The relationship between $\log k_{\text{cat}}/K_m$ (avge) and E^{1_7} of nitroaromatics is described by Equation (A1):

$$\log k_{\text{cat}}/K_m \text{ (avge)} = (8.64 \pm 0.30) + (11.47 \pm 0.94) E^{1_7}, \quad (A1)$$

$$r^2 = 0.9209, F(1,13) = 150.11.$$

Appendix B

We have shown that the cytotoxicity of model nitroaromatic compounds without alkylating groups towards MH22a and HCT-116 cells increases with their E^{1_7} and $\log D$ values [31,40]. Table A2 presents our previous data, supplemented by studies of some new compounds or repeated studies of some previously studied compounds. For quantitative analysis, data obtained in the current work were used when available.

Table A2. Single-electron reduction midpoint potentials of nitroaromatic compounds (E^{1_7}), their octanol/water distribution coefficients at pH 7.0 ($\log D$), and their concentrations causing 50% death of MH22a cells (cL_{50}) or inhibiting the growth of HCT-116 cells by 50%.

No.	Compound	E^{1_7} (V)	$\log D$	MH22a cL_{50} (μM)	HCT-116 GI_{50} (μM)
1	Nitrobenzene	−0.485	1.91	1800 ± 200	≥5000
2	4-Nitrobenzoic acid	−0.425	−1.66	≥6000	≥6000
3	2-Nitrothiophene	−0.390	1.86	341 ± 42	600 ± 70 ^a
4	4-Nitroacetophenone	−0.355	1.47	239 ± 19	400 ± 80
5	1,3-Dinitrobenzene	−0.345	1.85	130 ± 14	350 ± 20
6	4-Nitrobenzaldehyde	−0.325	1.63	200 ± 15	50.0 ± 6.0
7	2-Nitrothiophene-5-carboxymorpholide	−0.305	1.07	82.0 ± 12	n.d.
8	1,2-Dinitrobenzene	−0.287	1.85	25.4 ± 3.0	60.0 ± 10.0
9	2-Nitrothiophene-5-aldoxime	−0.280	1.7	145 ± 30 118 ± 20 ^a	20.0 ± 5.0
10	2-Nitrothiophene-5-aldehyde	−0.260	1.26	42.0 ± 5.0	20.0 ± 3.0 ^a
11	Nitrofurantoin	−0.255	−0.25	387 ± 25 320 ± 25 ^a	60.0 ± 10.0
12	Nifuroxime	−0.255	−0.34	40.5 ± 5.0	70.0 ± 10.0
13	1,4-Dinitrobenzene	−0.255	1.85	12.0 ± 1.5	40.0 ± 7.0
14	2,4,6-Trinitrotoluene	−0.253	2.31	17.4 ± 2.0	40.0 ± 8.0
15	Tetryl	−0.191	1.38	7.0 ± 1.0	8.0 ± 1.5

^a Data from this work.

The relationship between $\log cL_{50}$ towards MH22a cells and E^{1_7} of nitroaromatic compounds is described by Equation (A2):

$$\log cL_{50} = -(0.27 \pm 0.32) - (8.55 \pm 0.94) E^{1_7} - (0.29 \pm 0.07) \log D, \quad (A2)$$

$$r^2 = 0.9011, F(2,12) = 54.67.$$

The relationship between $\log GI_{50}$ towards MH22a cells and E^{1_7} of nitroaromatic compounds is described by Equation (A3):

$$\log GI_{50} = -(0.83 \pm 0.28) - (10.03 \pm 0.82) E^{1_7} - (0.17 \pm 0.06) \log D, \quad (A3)$$

$$r^2 = 0.9372, F(2,11) = 82.10.$$

References

- Patterson, S.; Fairlamb, A.H. Current and future prospects of nitro-compounds as drugs for trypanosomiasis and leishmaniasis. *Curr. Med. Chem.* **2019**, *26*, 4454–4475. [[CrossRef](#)] [[PubMed](#)]
- Hartkoorn, R.C.; Ryabova, O.B.; Chiarelli, L.R.; Riccardi, G.; Makarov, V.; Cole, S.T. Mechanism of action of 5-nitrothiophenes against *Mycobacterium tuberculosis*. *Antimicrob. Agents Chemother.* **2014**, *58*, 2944–2947. [[CrossRef](#)]
- Andrade, J.K.E.; Souza, M.I.F.; Gomes Filho, M.A.; Silva, D.M.F.; Barros, A.L.S.; Rodrigues, M.D.; Silva, P.B.N.; Nascimento, S.C.; Aguiar, J.S.; Brondani, D.J.; et al. *N*-pentyl-nitrofurantoin induces apoptosis in HL-60 leukemia cell line by upregulating BAX and downregulating BCL-xL gene expression. *Pharmacol. Rep.* **2016**, *68*, 1046–1053. [[CrossRef](#)]

4. Fielden, E.M.; Adams, G.E.; Cole, S.; Naylor, M.A.; O'Neill, P.; Stephens, M.A.; Stratford, I.J. Assessment of a range of novel nitro-aromatic radiosensitizers and bioreductive drugs. *Int. J. Radiat. Oncol. Biol. Phys.* **1992**, *22*, 707–711. [[CrossRef](#)]
5. Nepali, K.; Lee, H.-J.; Liou, J.-P. Nitro-group-containing drugs. *J. Med. Chem.* **2019**, *62*, 2851–2893. [[CrossRef](#)] [[PubMed](#)]
6. Orna, M.; Mason, R. Correlation of kinetic parameters of nitroreductase enzymes with redox properties of nitroaromatic compounds. *J. Biol. Chem.* **1989**, *264*, 12379–12384. [[CrossRef](#)]
7. Vidakovic, M.; Crossnoe, C.R.; Neidre, C.; Kim, K.; Krause, K.L.; Germanas, J.P. Reactivity of reduced [2Fe-2S] ferredoxin parallels host susceptibility to nitroimidazoles. *Antimicrob. Agents Chemother.* **2003**, *47*, 302–308. [[CrossRef](#)] [[PubMed](#)]
8. Wang, J.; Guise, C.P.; Dachs, G.U.; Phung, Y.; Lambie, N.K.; Patterson, A.V.; Wilson, W.R. Identification of one-electron reductases that activate both the hypoxia prodrug SN30000 and diagnostic probe EF5. *Biochem. Pharmacol.* **2014**, *91*, 436–446. [[CrossRef](#)]
9. Knox, R.J.; Friedlos, F.; Boland, M. The bioactivation of CB1954 and its use as a prodrug in antibody-directed enzyme prodrug therapy. *Cancer Metastasis Rev.* **1993**, *12*, 195–212. [[CrossRef](#)]
10. Šarlauskas, J.; Dičkanaitė, E.; Nemeikaitė, A.; Anusevičius, Ž.; Nivinskas, H.; Segura-Aguilar, J.; Čėnas, N. Nitrobenzimidazoles as substrates for DT-diaphorase and redox cycling compounds: Their enzymatic reactions and cytotoxicity. *Arch. Biochem. Biophys.* **1997**, *346*, 219–229. [[CrossRef](#)]
11. Le Campion, L.; Delaforge, M.; Noel, J.P.; Ouazzani, J. Metabolism of ¹⁴C-labelled 5-nitro-1,2,4-triazol-3-one by rat liver microsomes. Evidence for the participation of cytochromes P450. *Eur. J. Biochem.* **1996**, *248*, 401–406. [[CrossRef](#)]
12. Li, H.; Lin, D.; Peng, Y.; Zheng, J. Oxidative bioactivation of nitrofurantoin in rat liver microsomes. *Xenobiotica* **2017**, *47*, 103–111. [[CrossRef](#)]
13. Čėnas, N.; Nemeikaitė-Čėnienė, A.; Kosychova, L. Single- and two-electron reduction of nitroaromatic compounds by flavoenzymes: Implications for their cytotoxicity. *Int. J. Molec. Sci.* **2021**, *22*, 8534. [[CrossRef](#)]
14. Nordberg, J.; Arner, E.S. Reactive oxygen species, antioxidants, and the mammalian thioredoxin system. *Free. Radic. Biol. Med.* **2001**, *31*, 1287–1312. [[CrossRef](#)] [[PubMed](#)]
15. Lincoln, D.T.; Ali Emadi, E.M.; Tonissen, K.F.; Clarke, F.M. The thioredoxin-thioredoxin reductase system: Over-expression in human cancer. *Anticancer Res.* **2003**, *23*, 2425–2433.
16. Urig, S.; Becker, K. On the potential of thioredoxin reductase inhibitors for cancer therapy. *Semin. Cancer Biol.* **2006**, *16*, 452–465. [[CrossRef](#)] [[PubMed](#)]
17. Gencheva, R.; Arner, E.S.J. Thioredoxin reductase inhibition for cancer chemotherapy. *Annu. Rev. Pharmacol. Toxicol.* **2022**, *62*, 177–196. [[CrossRef](#)] [[PubMed](#)]
18. Lillig, C.H.; Holmgren, A. Thioredoxin and related molecules—From biology to health and disease. *Antioxid. Redox Signal.* **2007**, *9*, 25–47. [[CrossRef](#)]
19. Arcscott, L.; Gromer, S.; Schirmer, R.; Becker, K.; Williams, C.H., Jr. The mechanism of thioredoxin reductase from human placenta is similar to the mechanisms of lipoamide dehydrogenase and glutathione reductase and is distinct from the mechanism of thioredoxin reductase from *Escherichia coli*. *Proc. Natl. Acad. Sci. USA* **1997**, *94*, 3621–3626. [[CrossRef](#)]
20. Nordberg, J.; Zhong, L.; Holmgren, A.; Arner, E.S. Mammalian thioredoxin reductase is irreversibly inhibited by dinitrohalobenzenes by alkylation of both the redox active selenocysteine and its neighboring cysteine residue. *J. Biol. Chem.* **1998**, *273*, 10835–10842. [[CrossRef](#)]
21. Čėnas, N.; Prast, S.; Nivinskas, H.; Šarlauskas, J.; Arner, E.S.J. Interactions of nitroaromatic compounds with the mammalian selenoprotein thioredoxin reductase and the relation to induction of apoptosis in human cancer cells. *J. Biol. Chem.* **2006**, *281*, 5593–5603. [[CrossRef](#)] [[PubMed](#)]
22. Busker, S.; Page, B.; Arner, E.S.J. To inhibit TrxR1 is to inactivate STAT-3 inhibition of TrxR1 enzymatic function by STAT3 small molecule inhibitors. *Redox Biol.* **2020**, *36*, 101646. [[CrossRef](#)] [[PubMed](#)]
23. Stafford, W.C.; Peng, X.; Olofsson, M.H.; Zhang, X.; Luci, D.K.; Lu, L.; Cheng, C.; Tresauges, L.; Dexheimer, T.S.; Coussens, N.P.; et al. Irreversible inhibition of cytosolic thioredoxin reductase 1 as a mechanistic basis for anticancer therapy. *Sci. Transl. Med.* **2018**, *10*, eaaf7444. [[CrossRef](#)] [[PubMed](#)]
24. Xia, Y.; Wang, G.; Jiang, M.; Liu, X.; Zhao, Y.; Song, Y.; Jiang, B.; Zhu, D.; Hu, L.; Zhang, Z.; et al. A novel biological activity of the STAT3 inhibitor Stattic in inhibiting glutathione reductase and suppressing the tumorigenicity of human cervical cancer cells via a ROS-dependent pathway. *Onco. Target. Ther.* **2021**, *14*, 4047–4060. [[CrossRef](#)]
25. Hodge, C.D.; Edwards, R.A.; Markin, C.J.; McDonald, D.; Pulvino, M.; Huen, M.S.; Zhao, J.; Spyrapoulos, L.; Hendzel, M.J.; Glover, J.N. Covalent inhibition of Ubc13 affects ubiquitin signaling and reveals active site elements important for targeting. *ACS Chem. Biol.* **2015**, *10*, 1718–1728. [[CrossRef](#)]
26. Pontrelli, P.; Oranger, A.; Barozzino, M.; Divella, C.; Conserva, F.; Fiore, M.G.; Rossi, R.; Papale, M.; Castellano, G.; Simone, S.; et al. Deregulation of autophagy under hyperglycemic conditions is dependent on increased lysine 63 ubiquitination: A candidate mechanism in the progression of diabetic nephropathy. *J. Mol. Med.* **2018**, *96*, 645–659. [[CrossRef](#)]
27. Ivanes, F.; Faccenda, D.; Gatliff, J.; Ahmed, A.A.; Cocco, S.; Cheng, C.H.; Allan, E.; Russell, C.; Duchon, M.R.; Campanella, M. the compound BTB06584 is an IF-1 dependent selective inhibitor of the mitochondrial F₁F₀-ATPase. *Br. J. Pharmacol.* **2014**, *171*, 4193–4206. [[CrossRef](#)]
28. Adams, G.E.; Clarke, E.D.; Jacobs, R.S.; Stratford, I.J.; Wallace, R.G.; Wardman, P.; Watts, M.E. Mammalian cell cytotoxicity of nitrocompounds: Dependence upon reduction potential. *Biochem. Biophys. Res. Commun.* **1976**, *72*, 824–829. [[CrossRef](#)]

29. Guissany, A.; Henry, Y.; Lougmani, N.; Hickel, B. Kinetic studies of four types of nitroheterocyclic radicals by pulse radiolysis: Correlation of pharmacological properties to decay rates. *Free Rad. Biol. Med.* **1990**, *8*, 173–189. [[CrossRef](#)]
30. Čėnas, N.; Nemeikaitė-Čėnienė, A.; Sergedienė, E.; Nivinskas, H.; Anusevičius, Ž.; Šarlauskas, J. Quantitative structure-activity relationships in single-electron reduction of nitroaromatic explosives: Implications for their cytotoxicity. *Biochim. Biophys. Acta* **2001**, *1528*, 31–38. [[CrossRef](#)]
31. Nemeikaitė-Čėnienė, A.; Marozienė, A.; Misevičienė, L.; Tamulienė, J.; Yantsevich, A.V.; Čėnas, N. Flavoenzyme-catalyzed single-electron reduction of nitroaromatic antiandrogens: Implications for their cytotoxicity. *Free Radic. Res.* **2021**, *55*, 246–254. [[CrossRef](#)] [[PubMed](#)]
32. Marcinkevičienė, J.; Čėnas, N.; Kulys, J.; Usanov, S.A.; Sukhova, N.M.; Selezneva, I.S.; Gryazev, V.F. Nitroreductase reactions of the NADPH–adrenodoxin reductase. *Biomed. Biochim. Acta* **1990**, *49*, 167–172. [[PubMed](#)]
33. Marcus, R.; Sutin, N. Electron transfers in chemistry and biology. *Biochim. Biophys. Acta* **1985**, *811*, 265–322. [[CrossRef](#)]
34. Wardman, P. Reduction potentials of one-electron couples involving free radicals in aqueous solutions. *J. Phys. Chem. Ref. Data* **1989**, *18*, 1637–1755. [[CrossRef](#)]
35. Tedeschi, G.; Chen, S.; Massey, V. DT-diaphorase. Redox potential, steady-state, and rapid reaction studies. *J. Biol. Chem.* **1995**, *270*, 1198–1204. [[CrossRef](#)] [[PubMed](#)]
36. Misevičienė, L.; Anusevičius, Ž.; Šarlauskas, J.; Čėnas, N. Reduction of nitroaromatic compounds by NAD(P)H:quinone oxidoreductase (NQO1): The role of electron-accepting potency and structural parameters in the substrate specificity. *Acta Biochim. Pol.* **2006**, *53*, 569–576.
37. Misevičienė, L.; Krikštopaitis, K.; Čėnas, N. The comparative study of redox properties of recombinant human and mitochondrial NADPH:thioredoxin reductases. *Chemija* **2022**, *33*, 40–45. [[CrossRef](#)]
38. Miškinienė, V.; Anusevičius, Ž.; Marozienė, A.; Kliukienė, R.; Nivinskas, H.; Šarlauskas, J.; Čėnas, N.; Becker, K. Tetryl as inhibitor and ‘subversive substrate’ for human erythrocyte glutathione reductase. In Proceedings of the 13th International Symposium of Flavins and Flavoproteins, Konstanz, Germany, 29 August–4 September 1999.
39. Egolf, R.A.; Heindel, N.D. The synthesis of aryl 4-nitro-5-imidazolyl sulfone radiation sensitizers sterically protected against glutathione reaction. *J. Heterocycl. Chem.* **1991**, *28*, 577–582. [[CrossRef](#)]
40. Nemeikaitė-Čėnienė, A.; Šarlauskas, J.; Jonušienė, V.; Misevičienė, L.; Marozienė, A.; Yantsevich, A.V.; Čėnas, N. QSARs in prooxidant mammalian cell cytotoxicity of nitroaromatic compounds: The roles of compound lipophilicity and cytochrome P-450- and DT-diaphorase catalyzed reactions. *Chemija* **2020**, *31*, 170–177. [[CrossRef](#)]
41. Lalazar, G.; Requena, D.; Ramos-Espiritu, L.; Ng, D.; Bhola, P.D.; De Jong, Y.P.; Wang, R.; Narayan, N.J.C.; Shebl, S.; Levin, S.; et al. Identification of novel therapeutic targets for fibrolamellar carcinoma using patient-derived xenografts and direct-from-patient screening. *Cancer Discov.* **2021**, *11*, 2544–2563. [[CrossRef](#)]
42. Boghdeh, N.; McGraw, B.; Barrera, M.D.; Anderson, C.; Baha, H.; Risner, K.H.; Ogungbe, I.V.; Alem, F. Inhibitors of the ubiquitin-mediated signaling pathway exhibit broad-spectrum antiviral activities against New World alphaviruses. *Viruses* **2023**, *15*, 655. [[CrossRef](#)] [[PubMed](#)]
43. Miliukienė, V.; Čėnas, N. Cytotoxicity of nitroaromatic explosives and their biodegradation products in mice splenocytes: Implications for their immunotoxicity. *Z. Naturforsch. C* **2008**, *63*, 519–525. [[CrossRef](#)] [[PubMed](#)]
44. Sabatier, P.; Beusch, C.M.; Gencheva, R.; Cheng, Q.; Zubarev, R.; Arner, E.S.J. Comprehensive chemical proteomics analyses reveal that the new Tri-1 and Tri-2 compounds are more specific thioredoxin reductase 1 inhibitors than auranofin. *Redox Biol.* **2021**, *48*, 102184. [[CrossRef](#)] [[PubMed](#)]
45. Johnson, F.D.; Ferrarone, J.; Liu, A.; Brandstädter, C.; Munuganti, R.; Farnsworth, D.A.; Lu, D.; Luu, J.; Sihota, T.; Jansen, S.; et al. Characterization of a small molecule inhibitor of disulfide reductases that induces oxidative stress and lethality in lung cancer cells. *Cell Rep.* **2022**, *38*, 110343. [[CrossRef](#)]
46. Fritz-Wolf, K.; Urig, S.; Becker, K. The structure of human thioredoxin reductase 1 provides insight into C-terminal rearrangements during catalysis. *J. Mol. Biol.* **2007**, *370*, 116–127. [[CrossRef](#)]
47. Marozienė, A.; Lesanavičius, M.; Davioud-Charvet, E.; Aliverti, A.; Grellier, P.; Šarlauskas, J.; Čėnas, N. Antiplasmodial activity of nitroaromatic compounds: Correlation with their reduction potential and inhibitory action on *Plasmodium falciparum* glutathione reductase. *Molecules* **2019**, *24*, 4509. [[CrossRef](#)]
48. Sun, S.; Xu, W.; Zhang, Y.; Yang, Y.; Ma, Q.; Xu, J. Menadione inhibits thioredoxin reductase 1 via arylation of the Sec⁴⁹⁸ residue and enhances both NADPH oxidation and superoxide production in Sec⁴⁹⁸ to Cys⁴⁹⁸ substitution. *Free Rad. Biol. Med.* **2021**, *172*, 482–489. [[CrossRef](#)]
49. Wang, H.; Jiang, H.; Corbet, C.; de Mey, S.; Law, K.; Gevaert, T.; Feron, O.; De Ridder, M. Piperlongumine increases sensitivity of colorectal cancer cells to radiation: Involvement of ROS production via dual inhibition of glutathione and thioredoxin systems. *Cancer Lett.* **2019**, *450*, 42–52. [[CrossRef](#)]
50. Pechurskaja, T.A.; Harnastai, I.N.; Grabovec, I.P.; Gilep, A.A.; Usanov, S.A. Adrenodoxin supports reactions catalyzed by microsomal steroidogenic cytochrome P450s. *Biochem. Biophys. Res. Commun.* **2007**, *353*, 598–604. [[CrossRef](#)]
51. Becker, K.; Gui, M.; Schirmer, R.H. Inhibition of human glutathione reductase by S-nitrosoglutathione. *Eur. J. Biochem.* **1995**, *234*, 472–478. [[CrossRef](#)]

52. Rackham, O.; Shearwood, A.-M.; Thyer, R.; McNamara, E.; Davies, S.M.; Callus, B.A.; Miranda-Vizueté, A.; Berniers-Price, S.J.; Cheng, Q.; Arnér, E.S.; et al. Substrate and inhibitor specificities differ between human cytosolic and mitochondrial thioredoxin reductases: Implications for development of specific inhibitors. *Free Rad. Biol. Med.* **2011**, *50*, 689–699. [[CrossRef](#)] [[PubMed](#)]
53. Prochaska, H.J. Purification and crystallization of rat liver NAD(P)H:quinone-acceptor oxidoreductase by cibacron blue affinity chromatography: Identification of a new and potent inhibitor. *Arch. Biochem. Biophys.* **1988**, *267*, 529–538. [[CrossRef](#)] [[PubMed](#)]
54. Bacon, J.R.; Demas, J.N. Phase-plane and Guggenheim methods for treatment of kinetic data. *Anal. Chem.* **1997**, *55*, 653–656. [[CrossRef](#)]
55. Ito, M. Microassay for studying anticellular effects of human interferons. *J. Interferon. Res.* **1984**, *4*, 603–608. [[CrossRef](#)]
56. Hill, K.E.; McCollum, G.W.; Burk, R.F. Determination of thioredoxin reductase activity in rat liver supernatant. *Anal. Biochem.* **1997**, *253*, 123–125. [[CrossRef](#)]
57. Breccia, A.; Busi, F.; Gattavechia, E.; Tamba, M. Reactivity of nitro-thiophene derivatives with electron and oxygen radicals studied by pulse radiolysis and polarographic techniques. *Radiat. Environ. Biophys.* **1990**, *29*, 153–160. [[CrossRef](#)]

Disclaimer/Publisher’s Note: The statements, opinions and data contained in all publications are solely those of the individual author(s) and contributor(s) and not of MDPI and/or the editor(s). MDPI and/or the editor(s) disclaim responsibility for any injury to people or property resulting from any ideas, methods, instructions or products referred to in the content.